ISSN 1392 - 1207. MECHANIKA. 2012 Volume 18(2): 227-232

Metallurgical and composition analysis of melted marks due to electrical failures

Ying Wu*, Decai Han**

**Key laboratory of fire scene investigation and evidence identification, Ministry of Public Security, PR China, Shenyang Fire Research Institution, Ministry of Public Security, 110034, China, E-mail: yingw78@sina.com*

***Shenyang Gas Cylinder Safety Technology Co., Ltd., China*

crossref http://dx.doi.org/10.5755/j01.mech.18.2.1558

1. Introduction

Uncontrolled fire can devastate our assets and production sources, and this relates to the societal costs of fire prevention and loss restoration. The effects of fire on people and the environment become social issues that depend on the political ideology and economics that prevail in the state. The steps involved in the investigation of a fire are site examination and the selection, examination and testing of samples, collection of background data, and reconstruction and analysis. Electrical distribution wires with melted ends showing beaded, drop-shaped are frequently encountered after fires. These melted copper wires residues can provide fire investigators and forensic scientists with useful information on the progress of a fire even though they do not result from these cause.

Optical microscope has been commonly used for visual inspection of the microstructure, in which properties like porosity and cross-sectional metallurgical phases of the arc beads are investigated. Some other means of physical or chemical testing, such as simple visual observation of the macrostructure, secondary ion mass spectrometry (SIMS) and dendrite arm spacing (DAS) methods, have been proposed to analysis the melting mark of copper wires residues found in fire scenes [1-8]. However, most of the methods only entail subjective, qualitative criteria for distinguishing between beads that did or did not start a fire. Due to both further sensitivity of the instrument and the precision of chemical state determination of X-ray photoelectron spectroscopy (XPS) [9-16], XPS has been included to deal with insulating samples.

Copper oxide (i.e., CuO and Cu_2O) compounds are interesting materials because of their use as catalysts, interconnects in electronics, corrosion of alloys, etc. The identification of the actual oxidation state of copper in these systems is critical to understand their chemical behavior and physical properties. Usually, the attribution of oxidation states of this element is done by considering both the Cu 2p photoemission peaks and the X-ray induced Auger lines of copper (Cu LMM). In particular, the use of these two peaks is necessary if Cu+ has to be differentiated from Cu0. When copper oxides are dispersed on the surface of another oxide support, the electronic parameters of the Cu2+ or Cu+ species may undergo significant changes.

With present work, we carry out a further study on the some macroscopic observation, composition and microstructures of primary melted marks (PMM) and secondary melted marks (SMM) by video microscopes, X-ray photoelectron spectroscopy (XPS) and optical microscopes. As a result, the given fire cause is the integrative judgments of these methods results.

2. Experiments

2.1. Materials

PVC-coated wires (Ø = 0.75 mm^2) were used to form primary and secondary arc beads. There are many causes, processes and kinds of arc beads. In this experiment, however, the primary arc beads that were formed between two PVC-wounded copper wires in a half-obturator, when brought in contact with each other. The covering of the wire was burnt by the petrolic burner flames, and the two wires were short-circuited in the half-obturator to form secondary arc beads. The heating process used was an attempt to simulate the real fire during the accident.

2.2. XPS and data processing

XPS spectra were recorded in an ESCALAB 250 spectrometer from VG supplied with a preparation chamber (base pressure 10-8 Torrs) where all the evaporation and adsorption experiments were carried out. The spectra were recorded with the Al Kα (1486.6 eV) radiation in the constant pass energy mode with a value of 50 eV. In this way, the small displacements (less than 1 eV) of the peaks in energy position due to charging effects were compensated. In some cases, when the difference in BEs between the peaks was very small, their exact position was determined by fitting a Gaussian curve to them. A maximum error bar of 0.05 eV can be estimated for the measurements.

At least three independent measurements were carried out on the samples and the accuracy of the measured binding energies was estimated as ±0.1 eV. The instrument was calibrated according to the procedure reported in the literature [17]. Cu, C and O XPS spectra were detected as described in detail [18, 19]. The Cu 2p3/2 peak cannot be used to differentiate between Cu metal and cuprous oxide due to the small chemical shift between the two. The peak centre for both Cu and Cu_2O is located at a binding energy, Eb, of 932.5 eV (within 0.1 eV). These species can be differentiated on the basis of Cu LMM. Cuprous and cupric oxides can be distinguished in the photoelectron Cu 2p spectra, since cupric compounds show two strong shake-up peaks located approximately 10eV above the principal Cu 2p3/2 peak. So, in addition to the photoelectron lines examined in-depth analytical studies, special attention was paid to Cu LMM; their presence is due to the

relaxation of the excited states. One of the most useful concepts in XPS is the Auger parameter (α). This parameter can be related to the extra-atomic relaxation energy of photo-holes in the final state of the atoms undergoing photoemission. It depends on the electronic and dielectric properties of the environment around the photo excited atom. Within this context, we have also studied by XPS the changes in binding energy (BE) of the photoemission peaks and in the α' parameter of a cation. Based on these results, we can obtain the composition and the chemical state in the near-surface regions of PMM and SMM.

A correlation of such behavior with some macroscopic and metallurgical analysis of the PMM and SMM has been also studied.

2.3. Metallurgical analysis of PMM and SMM

The sample were mounted in resin and polished with emery paper and diamond paste. Subsequently, metallurgical analysis by visual inspection of the microstructure from the beads was recorded with a high-power magnification optical microscope.

3. Macrostructure analysis

In the investigation of fires, arc beads are frequently encountered because electricity is available in most buildings. Arc beads often assume a roughly-spherical shape (beaded) and drop-shaped shown as in Figs. 1, a and b. The shape however does not necessarily have to be spherical (beaded) or drop-shaped. Figs. 2, a and b give sunk and pointed shapes of arcs, respectively.

a

b

Fig. 1 Arc beads found in the fire debris

a

b

Fig. 2 Arc beads with irregular shapes

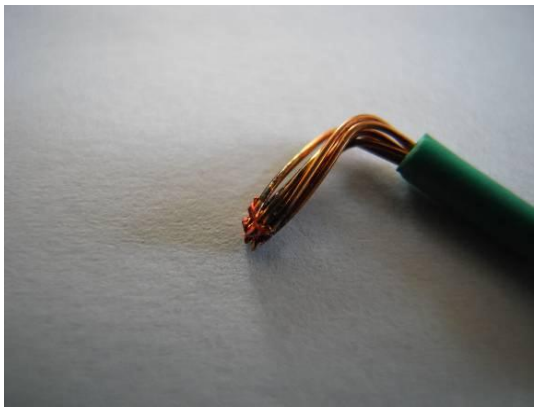

Fig. 3 A macroscopic views of PMM

Fig. 4 A macroscopic views of SMM

Figs. 3 and 4 give the macroscopic views of these experimented samples of PMM and SMM. While just simple visual observation is not sufficient for distinguishing two types of arc beads –'cause' and 'victim' beads. Consequently, X-ray photoelectron spectroscopy technique has been proposed.

4. Composition analysis

From the survey spectra (not shown), the presence of the elements copper, carbon and oxygen was detected on all the samples, as described elsewhere [17, 18]. In addition to the photoelectron lines examined in-depth analytical studies; special attention was paid to the X-ray induced Cu LMM; their presence is due to the relaxation of the excited states. We studied composition and the chemical state in the near-surface region of PMM and SMM.

4.1. Depth profiling results

The Cu LMM spectra were observed at 569.7±0.15 eV in the near-surface regions of PMM, while at 568.1±0.15 eV in the deeper depth of copper substrate (Fig. 5). On the other hand, Cu LMM spectra are 568.35±0.1 eV both in the near-surface regions of SMM and in the deeper depth of copper substrate (Fig. 6).

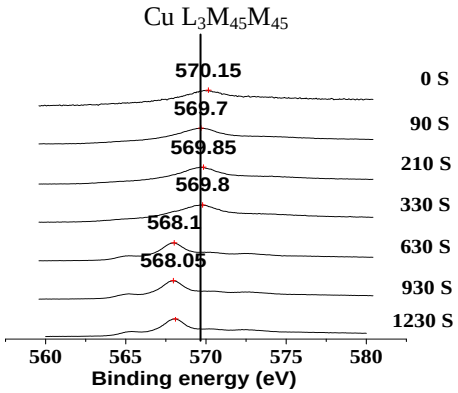

Fig. 5 X-ray induced Cu LMM Auger spectra recorded at different depths of the layer formed on PMM.

A depth vs. concentration profile has been made by progressively etching away portions of the surface and examining a lower layer. The quantitative results from the depth profiles of PMM and SMM are shown in Figs. 7 and 8. Carbon is present only as a subsurface contaminant and almost disappears after the first minute of sputtering in PMM. The oxygen concentration at the surface of PMM was with gentle increase till 42 nm but gradually decrease in the range of 42-66 nm and then showed drastic decrease (Fig. 7). On the other hand the concentration of carbon at the surface of SMM was also observed to be high, and then gradually diminished concentration of C was observed whereas higher as compared to PMM in the residual depth. The concentration of O at the surface of SMM showed gradually decrease throughout the depth profile (Fig. 8).

4.2. Chemical state plot

Combining the kinetic energy of the X-ray induced Auger lines and the binding energy of the photoelectron lines of the same element in a two-dimensional plot, the Wagner chemical state plot [19], a powerful tool for determining the chemical state, is obtained. This plot has found numerous applications in the investigation of geological materials [20]. Indeed, if both the binding energy of the photoelectron and the kinetic energy of the Auger electron are measured, a new parameter known as the Auger parameter (α') can be determined. The use of the Auger parameter concept permits obtaining more information from the joint analysis of the Auger and photoelectron lines rather than from either of them separately. Wagner originally defined the Auger parameter as the difference between the kinetic energy of the most intense Auger line and the most intense photoelectron line, making reference to the Fermi level rather than the vacuum level. The definition of the Auger parameter α' [21] used most frequently is

$$\alpha' = \alpha + h\nu$$

that is $\alpha' = KE_A + BE_p$

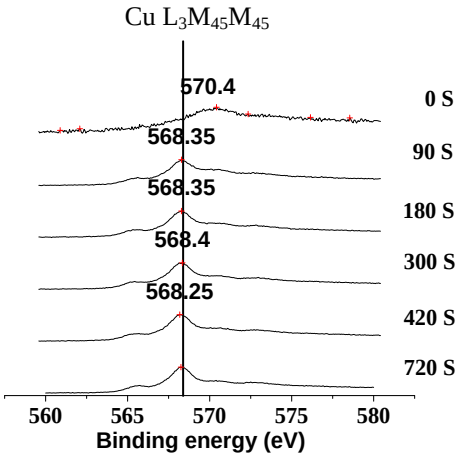

Fig. 6 X-ray induced Cu LMM Auger spectra recorded at different depths of the layer formed on SMM

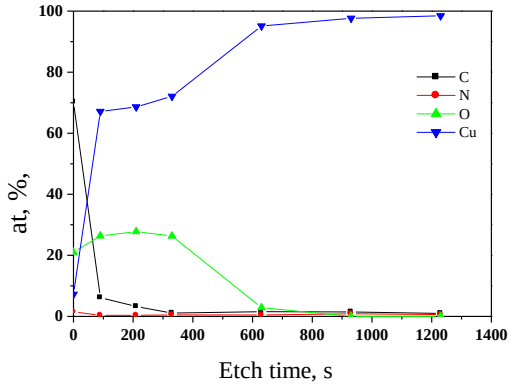

Fig. 7 XPS depth profiles of PMM

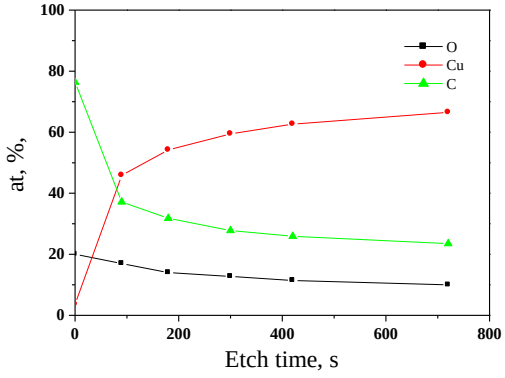

Fig. 8 XPS depth profiles of SMM

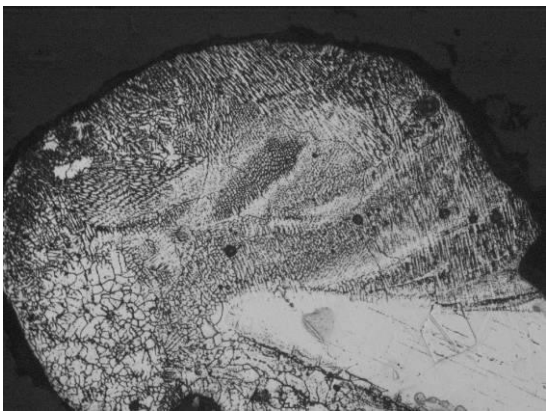

Fig. 9 A typical microstructure of PMM

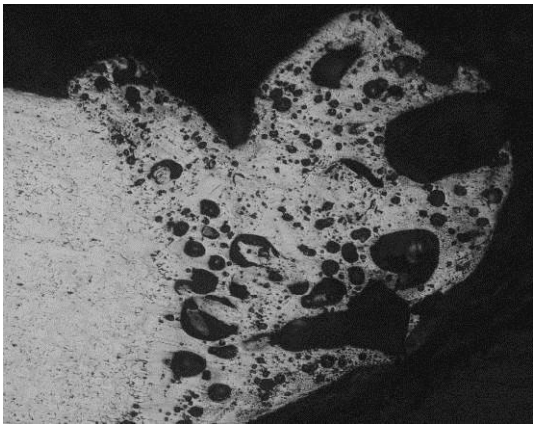

Fig. 10 A typical microstructures of SMM

The modified parameter α' as defined above is then independent of hν and always positive, and it is the sum of the kinetic energy of the Auger signal and the binding energy of the photoelectron line. This sum will be the same, independent of sample charging, and is found in the chemical state plot as a series of diagonal lines representing equal Auger parameters. The chemical state plot for PMM shows that the data points in the depth range of 18-66 nm with an Auger parameter of 1849.0 ± 0.15 eV, close to the value of Cu_2O. The data points in the depth range of 66-246 nm of PMM with an Auger parameter of 1850.8± 0.2 eV, similar to Cu metal (Table 1).

Table 1

Binding energy and Auger kinetic energy of copper Cu 2p3/2 and Cu LMM signals of copper compounds with the Auger parameter for PMM

Depth, nm	Cu 2p3/2 *BE*, eV	Cu $L_3M_{45}M_{45}$ *KE*, eV	α', eV	Compound
18	932.2	916.9	1849.1	Cu_2O
42	932.1	916.75	1848.85	Cu_2O
66	932.2	916.8	1849	Cu_2O
126	932.5	918.5	1851	Cu
186	932.45	918.3	1850.75	Cu
246	932.45	918.3	1850.75	Cu

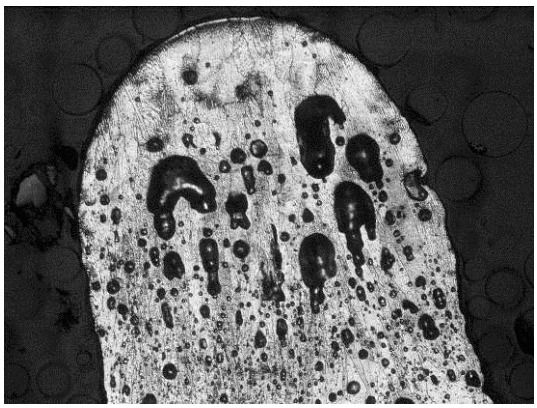

Fig. 11 A microstructure of PMM due to electric failures

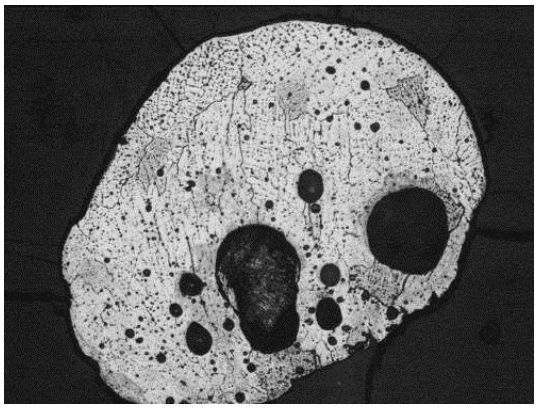

Fig. 12 A microstructure of SMM due to electric failures

The chemical state plot for SMM shows that the all data points throughout the depth profile with an Auger parameter of 1849.0 ± 0.15 eV, close to the value of Cu metal (Table 2).

Table 2

Binding energy and Auger kinetic energy of copper Cu 2p3/2 and Cu LMM signals of copper compounds with the Auger parameter for SMM

Depth, nm	Cu 2p3/2 *BE*, eV	Cu $L_3M_{45}M_{45}$ *KE*, eV	α', eV	Compound
18	932.75	918.25	1851	Cu
36	932.7	918.25	1850.95	Cu
60	932.75	918.2	1850.95	Cu
84	932.7	918.35	1851.05	Cu
144	932.7	918.35	1851.05	Cu

As a result, the film formed in PMM is constituted mainly of CuO_2. It thickness is estimated to be 66 nm. While the subsurface layer of molten product on SMM is not present CuO_2.

5. Metallurgical analysis

A typical cross-section of PMM in Fig. 9 possesses a sharp demarcation between a roughly-spherical bead and the fine cylindrical portion of the wire, and has little and small voids in melted part, while that of SMM (Fig. 10) does not show a sharp transition between molten and virgin material, a roughly cylindrical portion of the

wire with much and large voids in melted part.

Optical microscope has been commonly used for visual inspection of the microstructure of the fire copper wire debris in fire investigation, but in some cases, PMM and SMM are difficultly identified just using this method, even fallibly giving a false result, these experimental results shown as Figs. 11 and 12. So the results obtained from visual inspection are prone to human bias as it needs a skillful analyst and the results may vary with sample preparation and interpretation. In this situation, however, we can use the presence of Cu_2O and its quantitative results to identify these electric short circuit beads to be either the cause of a fire (a PMM) or one caused by the flames of the fire (a SMM), as complementary technique for judgments of fire cause.

6. Conclusion

Based on the macroscopic observation, XPS and metallurgical results the following conclusions can be drawn:

1. Electrical distribution wires with melted ends show not only roughly-spherical (beaded), drop-shaped, and pointed shapes, but also sunk and pointed ones. Just simple visual observation is not sufficient for distinguishing two types of arc beads – 'cause' and 'victim' beads.

2. The molten product on a PMM can be distinguished as three portions: surface layer with drastic decrease of carbon content; intermediate layer with gentle change of oxygen content, gradually diminished carbon peak, and consisted of Cu_2O; transition layer without Cu_2O and with rapid decrease of oxygen content. While the molten product on a SMM can be distinguished as two portions: surface layer with carbon content decreasing quickly; subsurface layer without Cu_2O and with carbon, oxygen content decreasing gradually. In addition, the presence of Cu_2O and the quantitative results can be used to identify these electric short circuit beads to be either the cause of a fire (a PMM) or one caused by the flames of the fire (a SMM), as complementary technique for judgments of fire cause.

3. A typical microstructure of PMM possesses a sharp demarcation between a roughly-spherical bead and the fine cylindrical portion of the wire, and has little and small voids in melted part, while that of SMM does not show a sharp transition between molten and virgin material, a roughly cylindrical portion of the wire with much and large voids in melted part. As a result, there was an obvious interface between the layered surface product and the substrate for the PMM, while as to SMM there was no interface.

Acknowledgment

This work was supported by Project 2009ZDYJSYXF027 of Key Research Program of Ministry of Public Security, PR China.

References

1. **Chen, C.Y.; Ling, Y.C.; Wang, J.T.; Chen, H.Y.** 2003. SIMS depth profiling analysis of electrical arc residues in fire investigation, Applied Surface Science 203-204: 779-784. http://dx.doi.org/10.1016/S0169-4332(02)00817-6.
2. **Bemand B.** 1994. Examination of arc beads, Fire Arson Invest, 44(4): 20-22.
3. **Satoh, K.; Sugisaki, M.; Kakizaki, S.; Itoh, C.; Saitoh, K.; Iwaki, M.** 1996. Secondary ion mass spectroscopy (SIMS) and auger electron spectroscopy (AES) applied to the fire investigation for short circuit, In Proc. 1996 Annual Mtg. of Japan Assn. for Fire Science and Engrg. 282-285.
4. **Wang Xi-qing; Han Baoyu; Di Man.** 1997. Guidance for Electric Fire Scene Survey and Identification Technique. Shenyang: Liaoning University Publishing Company.
5. **Lee, E.-P.; Ohtani, H.; Matsubara, Y.; Seki, T.; Hasegawa, H.; Imada, S.** 1999. Study on primary and secondary molten marks, In Proc. 1st Conf. Assn. Korean-Japanese Safety Engineering Society, Korean Institute for Industrial Safety. 209-212.
6. **Lee, E.-P.; Ohtani, H.; Matsubara, Y.; Seki, T., Hasegawa, H., Imada, S.; Yashiro, I.** 2000. Study on discrimination between primary and secondary molten marks by analyzing the crystal structure of the carbon in carbonized residue, Bulletin of Japan Association for Fire Science and Engineering, 50(2): 31-40 (in Japanese).
7. **Lee, E.-P.; Ohtani, H.; Seki, T.; Hasegawa, H.; Imada, S.; Yashiro, I.** 2000. Study on discrimination between primary and secondary molten marks by DAS, Bulletin of Japan Association for Fire Science and Engineering, 50(1): 1-12 (in Japanese).
8. **Chen, C.Y.; Ling, Y.C.; Wang, J.T.; Chen, H.Y.** 2003. SIMS depth profiling analysis of electrical arc residues in fire investigation, Applied Surface Science, 203-204: 779-784. http://dx.doi.org/10.1016/S0169-4332(02)00817-6.
9. **Zhong Yong-qiang; Zheng Jia-gui; Feng Liang-heng; Cai Wei; CAI Ya-ping; Zhang Jing-quan; Li Bin; Lei Zhi; Li Wei; Wu Lili.** 2007. Study on ZnTe(ZnTe: Cu) polycrystalline films by XPS, Spectroscopy and Spectral Analysis, 27(3): 598-601.
10. **Fan Jin-chuan; Wu Hui; Huang Wei; Xie Ke-chang** 2008. Effect of surfactants on structure and performance of Cu-Zn-Al catalyst prepared by complete liquid-phase technology, Chemical Journal of Chinese Universities, 29(5): 993-999.
11. **Guo Xian-zhi; Huang Jing; Wang Yan-mei; Wang Shu-rong; Zhang Bao-long; Wu Shi-huang.** 2008. Preparation, characterization and CO oxidation catalytic properties of CuO /TiO_2 catalysts supported on porous microspheres composed of TiO_2 nanocrystals, Chemical Journal of Chinese Universities, 29(6): 1220-1223.
12. **Wang Dan-jun; Guo Li; Li Dong-sheng; Fu Feng; Wang Wen-liang; Yan Hong-tao.** 2008. Study on spectroscopic properties of CuO nanoparticles, Spectroscopy and Spectral Analysis, 28(4): 788-792.
13. **Song Hui-jin; Zheng Jia-gui; Feng Liang-heng; Zhang Jing-quan; Li Wei; Li Bing; Wu Lili; Lei Zhi; Yan Qiang.** 2008. Study on the back contact performances of CdTe solar cells by XPS, Spectroscopy and Spectral Analysis, 28(12): 2737-2740.
14. **Wang Jing-ming; Zheng Yong-mei; Jianng Lei.** 2008. bubble transfer effect of superhydrophobic mesh

structure in water, Chemical Journal of Chinese Universities, 29(12): 2484-2488.
15. **Fan Min-guang; Li Bin; Zhang Fei-yue; Li Wang-liang; Xing Jian-min; Liu Zi-li.** 2009. Distribution of copper ions in a CuLaHY zeolite and its performance in adsorption desulfurization, Acta Phys.-Chim. Sin., 25(3): 495-501.
16. **Ouyang Jian-ming; Bai Yu; Gui Yu et al.** 2004. XPS spectra of langmuir-blodgett films and their electroluminescence, Spectroscopy and Spectral Analysis, 24(4): 499-501.
17. **Rossi, A.; Atzei, D.; Da Pelo, S.; Frau, F.; Lattanzi, P.; England, K.E.R.; Vaughan, D.J.** 2001. Quantitative X ‐ ray photoelectron spectroscopy study of enargite (Cu3AsS4) surface, Surface and Interface Analysis. 31(6): 465-470. http://dx.doi.org/10.1002/sia.1072.
18. **Rossi, A.; Atzei, D.; Elsener, B.; Da Pelo, S.; Frau, F.; Lattanzi, P.; Wincott, P.L.; Vaughan, D.J.** 2001. Water–Rock Interaction, Cidu R (ed.). A.A. Balkema Publishers: Rotterdam, 1: 427.
19. **Wagner, C.D.; Joshi. A.** 1988. The auger parameter, its utility and advantages: a review, J. Electron Spectrosc. Relat. Phenom, 47: 283-313. http://dx.doi.org/10.1016/0368-2048(88)85018-7.
20. **Perry, D.L.; Taylor, J.A.; Wagner, C.D.** 1990. In Instrumental Surface Analysis of Geological Materials, Perry DL (ed.), VCH Publishers: Weinheim, 45p.
21. **Giuliano M.** 1998. Auger parameter and Wagner plot in the characterization of chemical states by X-ray photoelectron spectroscopy: a review, J. Electron Spectrosc. Relat. Phenom, 95(2-3): 95-144. http://dx.doi.org/10.1016/S0368-2048(98)00249-7.

Ying Wu, Decai Han

APLYDYMO MEDŽIAGOS METALURGINĖ IR CHEMINĖ ANALIZĖ VERTINANT ELEKTRINIUS PAŽEIDIMUS

R e z i u m ė

Po gaisro dažnai yra vertinami elektros laidai su aplydytais galais, turinčiais bortelius, lašo pavidalą ir užvartų. Tai gali suteikti naudingos informacijos apie gaisro priežastis ir išplitimą. Pirminiams aplydymo požymiams nustatyti, nurodant lanko susidarymą kaip gaisro priežastį, ir antriniams aplydymo požymiams nustatyti, nurodant lanko susidarymo kaip gaisro rezultatą, buvo išnagrinėti įvairūs metodai. Vienu metodu pirminį ir antrinį aplydymą nustatyti sunku. Straipsnyje yra atlikta šių reiškinių koreliacija naudojant mikroskopinę anglies ir deguonies kiekybinę analizę vielos skerspjūvyje, cheminės sudėties analizę paviršiui artimuose sluoksniuose ir metalurginę pirminio ir antrinio aplydymo medžiagos analizę. Gaisro priežasties nustatymas yra integralus šių tyrimų rezultatas.

Ying Wu, Decai Han

METALLURGICAL AND COMPOSITION ANALYSIS OF MELTED MARKS DUE TO ELECTRICAL FAILURES

S u m m a r y

Electrical distribution wires with melted ends showing beaded, drop-shaped, and pointed shapes are frequently encountered after fires, which may be provide useful information on the cause and development of the fire. Various methods have been studied for identifying between primary melted marks (PMM), indicating arcing as the cause of the fire, and secondary melted marks (SMM), indicating arcing as a result of the fire. But in some major cases, PMM and SMM are difficultly identified just using one method. In this study, a correlation of such behavior with some macroscopic, the in-depth composition of carbon and oxygen quantitative analysis, the composition and the chemical state in the near-surface regions, and metallurgical analysis of PMM and SMM has been studied. As a result, the given fire cause is the integrative judgments of these methods.

Keywords: metallurgical and composition analysis, melted marks, electrical failures.

Received March 23, 2011
Accepted March 08, 2012